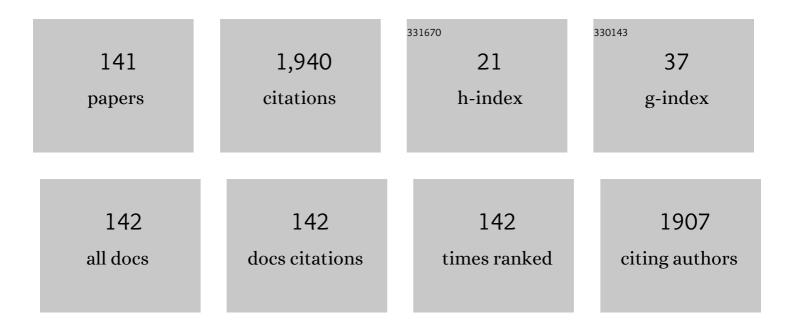
Seiichi Watanabe

List of Publications by Year in descending order

Source: https://exaly.com/author-pdf/4714615/publications.pdf Version: 2024-02-01



#	Article	IF	CITATIONS
1	CoCrFeNiTi-based high-entropy alloy with superior tensile strength and corrosion resistance achieved by a combination of additive manufacturing using selective electron beam melting and solution treatment. Materials Letters, 2017, 189, 148-151.	2.6	130
2	Synergistic effect of helium and hydrogen for defect evolution under multi-ion irradiation of Fe–Cr ferritic alloys. Journal of Nuclear Materials, 2004, 329-333, 294-298.	2.7	117
3	Hidden amorphous phase and reentrant supercooled liquid in Pd-Ni-P metallic glasses. Nature Communications, 2017, 8, 14679.	12.8	109
4	Controlled formation of metallic nanoballs during plasma electrolysis. Applied Physics Letters, 2007, 91, .	3.3	86
5	Sink effect of grain boundary on radiation-induced segregation in austenitic stainless steel. Journal of Nuclear Materials, 2000, 283-287, 152-156.	2.7	74
6	Mechanical and corrosion properties of CoCrFeNiTi-based high-entropy alloy additive manufactured using selective laser melting. Additive Manufacturing, 2019, 25, 412-420.	3.0	54
7	Tuning Optoelectrical Properties of ZnO Nanorods with Excitonic Defects via Submerged Illumination. Nano Letters, 2017, 17, 2088-2093.	9.1	51
8	Formation of CuO nano-flowered surfaces via submerged photo-synthesis of crystallites and their antimicrobial activity. Scientific Reports, 2017, 7, 1063.	3.3	49
9	Quantitative studies of irradiation-induced segregation and grain boundary migration in FeCrNi alloy. Journal of Nuclear Materials, 1995, 224, 158-168.	2.7	47
10	Radiation-induced segregation and corrosion behavior on Σ3 coincidence site lattice and random grain boundaries in proton-irradiated type-316L austenitic stainless steel. Journal of Nuclear Materials, 2013, 434, 65-71.	2.7	37
11	Atomic Structure of Faceted Σ3 CSL Grain Boundary in Silicon: HRTEM and &kl1>Ab-initio Calculation. Materials Transactions, 2007, 48, 2585-2589.	1.2	36
12	<i>In situ</i> observation of self-organizing nanodot formation under nanosecond-pulsed laser irradiation on Si surface. Journal of Applied Physics, 2010, 108, .	2.5	31
13	Surface cracking on Σ3, Σ9 CSL and random grain boundaries in helium implanted 316L austenitic stainless steel. Journal of Nuclear Materials, 2013, 432, 23-27.	2.7	31
14	Grain boundary engineering of austenitic steel PNC316 for use in nuclear reactors. Journal of Nuclear Materials, 2011, 414, 232-236.	2.7	30
15	In situ transmission electron microscopy observation of the decomposition of MgH2 nanofiber. International Journal of Hydrogen Energy, 2011, 36, 3600-3605.	7.1	28
16	Discriminant of RIS in multi-component alloys. Journal of Nuclear Materials, 1994, 208, 191-194.	2.7	27
17	A multi-scale approach to radiation-induced segregation at various grain boundaries. Journal of Nuclear Materials, 2004, 329-333, 1166-1169.	2.7	26
18	Effect of mechanical alloying parameters on irradiation damage in oxide dispersion strengthened ferritic steels. Journal of Nuclear Materials, 2000, 283-287, 647-651.	2.7	25

#	Article	IF	CITATIONS
19	Solution Plasma-Synthesized Black TiO ₂ Nanoparticles for Solar–Thermal Water Evaporation. ACS Applied Nano Materials, 2021, 4, 3940-3948.	5.0	25
20	In situ direct observation of photocorrosion in ZnO crystals in ionic liquid using a laser-equipped high-voltage electron microscope. AIP Advances, 2017, 7, .	1.3	24
21	Corrosion–erosion test of SS316L grain boundary engineering material (GBEM) in lead bismuth flowing loop. Journal of Nuclear Materials, 2012, 431, 91-96.	2.7	22
22	Size-Controlled Ni Nanoparticles Formation by Solution Glow Discharge. Journal of the Physical Society of Japan, 2010, 79, 083501.	1.6	21
23	Microstructure analysis of ion beam-induced surface nanostructuring of thin Au film deposited on SiO2 glass. Journal of Materials Science, 2013, 48, 920-928.	3.7	21
24	A pathway of nanocrystallite fabrication by photo-assisted growth in pure water. Scientific Reports, 2015, 5, 11429.	3.3	21
25	Heterogeneous dislocation formation and solute redistribution near grain boundaries in austenitic stainless steel under electron irradiation. Acta Materialia, 2001, 49, 1129-1137.	7.9	20
26	Effect of Surface Modification by Ion Implantation on Hydrogenation Property of TiFe Alloy. Materials Transactions, 2002, 43, 2703-2705.	1.2	20
27	Radiation-induced segregation accompanied by grain boundary migration in austenitic stainless steel. Journal of Nuclear Materials, 1996, 232, 113-118.	2.7	19
28	A new model for radiation-induced grain boundary segregation with grain boundary movement in concentrated alloy system. Journal of Materials Science, 2005, 40, 889-893.	3.7	19
29	Dislocation Loop Formation and Growth under In Situ Laser and/or Electron Irradiation. Scientific Reports, 2011, 1, 190.	3.3	19
30	Effects of nanosecond-pulsed laser irradiation on nanostructure formation on the surface of thin Au films on SiO2 glass substrates. Applied Surface Science, 2014, 289, 274-280.	6.1	19
31	Photochemistry and the role of light during the submerged photosynthesis of zinc oxide nanorods. Scientific Reports, 2018, 8, 177.	3.3	19
32	Fabrication of a Au/Si nanocomposite structure by nanosecond pulsed laser irradiation. Nanotechnology, 2011, 22, 375607.	2.6	18
33	Facile synthesis of ZnFe2O4/SnO2 composites for efficient photocatalytic degradation of methylene blue. Materials Chemistry and Physics, 2021, 262, 124273.	4.0	18
34	Effect of He on void formation and radiation-induced segregation in dual-beam irradiated Fe-Cr-Ni. Journal of Nuclear Materials, 1994, 212-215, 330-335.	2.7	16
35	Molten salt-assisted shape modification of CaFe2O4 nanorods for highly efficient photocatalytic degradation of methylene blue. Optical Materials, 2021, 119, 111295.	3.6	16
36	Effect of additional minor element on radiation-induced grain boundary segregation in austenitic stainless steel under electron irradiation. Nuclear Instruments & Methods in Physics Research B, 1999, 153, 142-146.	1.4	15

#	Article	IF	CITATIONS
37	On the mechanism of radiation-induced segregation. Journal of Nuclear Materials, 1997, 240, 251-253.	2.7	14
38	Present status of study on development of materials resistant to radiation and beam impact. Journal of Nuclear Materials, 2008, 377, 21-27.	2.7	14
39	Effect of hydrogen ion/electron dual-beam irradiation on microstructural damage of a 12Cr-ODS ferrite steel. Journal of Nuclear Materials, 2010, 398, 81-86.	2.7	14
40	Enhanced Magnetoâ€optical Properties of Semiconductor EuS Nanocrystals Assisted by Surface Plasmon Resonance of Gold Nanoparticles. Chemistry - A European Journal, 2013, 19, 14438-14445.	3.3	14
41	Fabrication of Nanoparticles by Electric Discharge Plasma in Liquid. Archives of Metallurgy and Materials, 2013, 58, 425-429.	0.6	14
42	lon irradiation synthesis of Ag–Au bimetallic nanospheroids in SiO2 glass substrate with tunable surface plasmon resonance frequency. Journal of Applied Physics, 2013, 114, .	2.5	14
43	Theory of superconductivity. 3. 2D conduction bands for high Tc. Bose-Einstein condensation transition of the third order. Journal of Superconductivity and Novel Magnetism, 1992, 5, 219-237.	0.5	13
44	Effects of Fast Reactor Irradiation Conditions on Tensile and Transient Burst Properties of Ferritic/Martensitic Steel Claddings. Journal of Nuclear Science and Technology, 2007, 44, 1535-1542.	1.3	13
45	Dislocation loop formation under various irradiations of laser and/or electron beams. Acta Materialia, 2013, 61, 2966-2972.	7.9	13
46	Evolution of 3D nanoporosity and morphology in selectively dealloying ternary Au ₅₅ Cu ₂₅ Si ₂₀ metallic glass ribbon with enhanced alcohol electro-oxidation performance. Nanoscale, 2018, 10, 18846-18856.	5.6	13
47	Atomistic study of structural fluctuations during radiation-induced amorphization in the ordered intermetallic compound NiTi. Philosophical Magazine Letters, 2001, 81, 789-794.	1.2	12
48	Development of advanced materials for spallation neutron sources and radiation damage simulation based on multi-scale models. Journal of Nuclear Materials, 2012, 431, 16-25.	2.7	12
49	Nanopatterns induced by pulsed laser irradiation on the surface of an Fe-Al alloy and their magnetic properties. Applied Physics Letters, 2013, 102, .	3.3	12
50	Synthesis of stainless steel nanoballs via submerged glow-discharge plasma and its photocatalytic performance in methylene blue decomposition. Journal of Experimental Nanoscience, 2015, 10, 965-982.	2.4	12
51	Galvanic-submerged photosynthesis of crystallites: Fabrication of ZnO nanorods@ Cu-surface. Applied Surface Science, 2019, 489, 313-320.	6.1	12
52	Boundary Structure of Mo/Si Multilayers for Soft X-Ray Mirrors. Japanese Journal of Applied Physics, 2002, 41, 3052-3056.	1.5	11
53	Effect of alloying elements and neutron-irradiation on hydrogen behavior in V alloys. Journal of Nuclear Materials, 2004, 329-333, 481-485.	2.7	11
54	Dynamic and static hydrogen effects on mechanical properties in pure vanadium. Journal of Nuclear Materials, 2004, 329-333, 477-480.	2.7	11

#	Article	IF	CITATIONS
55	Mechanical properties and microstructural stability of 11Cr-ferritic/martensitic steel cladding under irradiation. Journal of Nuclear Materials, 2010, 398, 59-63.	2.7	11
56	Luminescence properties of ZnO-M heterostructures fabricated by galvanic-submerged photosynthesis of crystallites. Applied Surface Science, 2019, 489, 269-277.	6.1	11
57	Defect-flow-induced grain boundary migration with segregation under electron irradiation. Ultramicroscopy, 1994, 56, 193-199.	1.9	10
58	Hydride formation and fracture of vanadium alloys. Journal of Nuclear Materials, 2002, 307-311, 625-629.	2.7	10
59	Microstructure and analysis of oxide scales formed on Cr–Si–Ni compacts in air and H2O-containing atmosphere. Corrosion Science, 2010, 52, 2098-2103.	6.6	10
60	Self-Organized Two-Dimensional <i>Vidro-Nanodot</i> Array on Laser-Irradiated Si Surface. Applied Physics Express, 2011, 4, 055202.	2.4	10
61	Photophysical properties of luminescent silicon nanoparticles surface-modified with organic molecules via hydrosilylation. Photochemical and Photobiological Sciences, 2016, 15, 99-104.	2.9	10
62	In-situ visualizing atomic structural evolution during crystallization in ternary Zr Cu Al bulk metallic glasses. Intermetallics, 2019, 105, 173-178.	3.9	10
63	Micro-chemical analysis of diffusion bonded W–SiC joint. Journal of Nuclear Materials, 2011, 417, 391-394.	2.7	9
64	Shift of localized surface plasmon resonance by Ar-ion irradiation of Ag–Au bimetallic films deposited on Al2O3 single crystals. Nuclear Instruments & Methods in Physics Research B, 2013, 314, 112-116.	1.4	9
65	Synthesis of yellow persistent phosphor garnet by mixed fuel solution combustion synthesis and its characteristic. Journal of Physics and Chemistry of Solids, 2020, 142, 109436.	4.0	9
66	On the angular dependence of the cyclotron resonance peaks in lead. Journal of Physics and Chemistry of Solids, 1991, 52, 985-989.	4.0	8
67	Concentration dependence of radiation-induced segregation in FeCrNi alloy. Journal of Nuclear Materials, 1995, 226, 330-331.	2.7	8
68	Effect of Ni and Cr concentration on grain boundary segregation in Feî—,Crî—,Ni alloys. Journal of Nuclear Materials, 1996, 239, 205-209.	2.7	8
69	Nano-crystalline formation during stress-induced amorphization at crack tips in TiNi. Journal of Electron Microscopy, 1999, 48, 613-616.	0.9	8
70	Microstructural development in a model austenitic alloy following electron and ion irradiation. Journal of Nuclear Materials, 2008, 382, 197-202.	2.7	8
71	A HRTEM and EELS study of Pd/ZnO polar interfaces. Philosophical Magazine, 2008, 88, 1493-1509.	1.6	8
72	3D Nanoporous Cold with Very Low Parting Limit Derived from Auâ€Based Metallic Glass and Enhanced Methanol Electroâ€oxidation Catalytic Performance Induced by Metal Migration. ChemNanoMat, 2018, 4, 88-97.	2.8	8

#	Article	IF	CITATIONS
73	The origin of opto-functional enhancement in ZnO/CuO nanoforest structure fabricated by submerged photosynthesis. Applied Materials Today, 2022, 26, 101359.	4.3	8
74	Temporal Fluctuation and Its Power Law in the Crystalline-To-Glass Transition During Electron Irradiation. Philosophical Magazine, 2003, 83, 2599-2619.	1.6	7
75	Metastable Defect Cluster Formation during Radiation-Induced Amorphization in NiTi. Materials Transactions, 2004, 45, 24-28.	1.2	7
76	EELS and <1>Ab-Initio 1 Study of Faceted CSL Boundary in Silicon. Materials Transactions, 2011, 52, 276-279.	1.2	7
77	The Irradiation Effect of a Simultaneous Laser and Electron Dual-beam on Void Formation. Scientific Reports, 2013, 3, 1201.	3.3	7
78	Radiation-induced segregation at grain boundary in Feî—,Crî—,Ni alloy system: effect of temperature variation. Journal of Nuclear Materials, 1996, 239, 200-204.	2.7	6
79	Theoretical prediction and direct observation of dislocation-free zone formation near a grain boundary in austenitic stainless steel under electron irradiation. Philosophical Magazine Letters, 1996, 74, 351-356.	1.2	6
80	Nanosecond pulsed laser induced self-organized nano-dots patterns on GaSb surface. Applied Surface Science, 2014, 307, 24-27.	6.1	6
81	Effect of laser and/or electron beam irradiation on void swelling in SUS316L austenitic stainless steel. Journal of Nuclear Materials, 2017, 488, 215-221.	2.7	6
82	Atmospherically sintered copper-base alloy application film with self-assembled barrier layer on silicon substrate for silicon photovoltaics. Journal of Alloys and Compounds, 2018, 757, 333-339.	5.5	6
83	Material Factors in the Decrepitation of Hydrogen Storage Alloys. Nippon Kinzoku Gakkaishi/Journal of the Japan Institute of Metals, 1999, 63, 601-604.	0.4	6
84	Mesoporous single crystal titanium oxide microparticles for enhanced visible light photodegradation. Optical Materials, 2022, 127, 112297.	3.6	6
85	Relationship between superconductivity and band structures of electrons and phonons. Journal of Superconductivity and Novel Magnetism, 1993, 6, 75-79.	0.5	5
86	Dynamical Study of Spatio-Temporal Structural Fluctuations in the Intermetallic Compound Nickel-Titanium during Radiation-Induced Crystalline-to-Amorphous Transformation. Materials Transactions, 2002, 43, 1716-1718.	1.2	5
87	Atomistic Analysis of Stress-induced Local Amorphization in NiTi Alloy. Radiation Effects and Defects in Solids, 2002, 157, 101-108.	1.2	5
88	Magnetic properties on the surface of FeAl stripes induced by nanosecond pulsed laser irradiation. Journal of Applied Physics, 2014, 115, 17B901.	2.5	5
89	In-situ observation of self-assembly of quasi-two-dimensional Au nano-submicron particles on β -SiC substrates via nanosecond-pulsed laser irradiation-induced dewetting of thin Au films. Materials Letters, 2016, 164, 202-205.	2.6	5
90	lon beam surface nanostructuring of noble metal films with localized surface plasmon excitation. Current Opinion in Solid State and Materials Science, 2017, 21, 177-188.	11.5	5

#	Article	IF	CITATIONS
91	Fabrication of Iron Oxide Nanoparticles via Submerged Photosynthesis and the Morphologies under Different Light Sources. ISIJ International, 2019, 59, 2352-2358.	1.4	5
92	Light and Shadow Effects in the Submerged Photolytic Synthesis of Micropatterned CuO Nanoflowers and ZnO Nanorods as Optoelectronic Surfaces. ACS Applied Nano Materials, 2020, 3, 1783-1791.	5.0	5
93	Selective fabrication of tungsten nano-oxides via submerged photosynthesis with hydrogen peroxide for chromic device application. Materials Letters, 2021, 302, 130344.	2.6	5
94	Photo- & radio-chromic iron-doped tungstic acids fabricated via submerged photosynthesis. Optical Materials, 2022, 124, 111966.	3.6	5
95	Atomistic observation and simulation analysis of spatio-temporal fluctuations during radiation-induced amorphization. Journal of Electron Microscopy, 2003, 52, 33-40.	0.9	4
96	Ion Implantation Induced Martensite Nucleation in SUS301 Steel. Materials Transactions, 2007, 48, 924-930.	1.2	4
97	In-situ Observation of Fracture Behavior on Nano Structure in NITE SiC/SiC Composite by HVEM. IOP Conference Series: Materials Science and Engineering, 2011, 18, 162013.	0.6	4
98	Plasmonic surface nanostructuring of Au-dots@SiO2via laser-irradiation induced dewetting. Nanotechnology, 2017, 28, 275701.	2.6	4
99	Visualization of aquaionic splitting via iron corrosion. Scientific Reports, 2020, 10, 1726.	3.3	4
100	On the conductance of a lattice-like network. Journal of Physics and Chemistry of Solids, 1989, 50, 27-31.	4.0	3
101	On the Orientation Dependence of the Cyclotron Resonance Peaks for Holes in Ge and Si. Physica Status Solidi (B): Basic Research, 1990, 158, K69.	1.5	3
102	A computational study of dislocation evolution and radiation-induced segregation at a grain boundary. Journal of Nuclear Materials, 1996, 239, 176-179.	2.7	3
103	Formation of sphalerite and wurtzite ZnO in Pd–Zn alloy after internal oxidation at elevated temperatures. Journal of Materials Science, 2011, 46, 4568-4573.	3.7	3
104	Effects of ion and nanosecond-pulsed laser co-irradiation on the surface nanostructure of Au thin films on SiO2 glass substrates. Journal of Applied Physics, 2014, 115, .	2.5	3
105	Anisotropic surroundings effects on photo absorption of partially embedded Au nanospheroids in silica glass substrate. AIP Advances, 2015, 5, .	1.3	3
106	Effect of Glass Frits Amount on Atmospheric Sintering Behavior and Characteristics of Electrode Produced by Copper–Phosphorus Alloy. IEEE Journal of Photovoltaics, 2015, 5, 1325-1334.	2.5	3
107	A reaction mechanism of atmospheric sintering for copper–phosphorus alloy electrode. Journal of Alloys and Compounds, 2017, 695, 3353-3359.	5.5	3
108	Effects of Fast Reactor Irradiation Conditions on Tensile and Transient Burst Properties of Ferritic/Martensitic Steel Claddings. Journal of Nuclear Science and Technology, 2007, 44, 1535-1542.	1.3	3

#	Article	IF	CITATIONS
109	Theory of the anisotropies in the cyclotron resonance peaks for electrons in Ge based on hexagonal orbitals. Solid State Communications, 1989, 72, 581-583.	1.9	2
110	Effect of additional minor elements on void nucleation in stainless steels during simultaneous irradiation with helium ions and electrons. Journal of Nuclear Materials, 1996, 233-237, 177-182.	2.7	2
111	Theoretical and Experimental Studies of Irradiation-Induced Grain Boundary Migration Depending on Orientation. Materials Science Forum, 1996, 207-209, 561-564.	0.3	2
112	Numerical Simulation of Solidified Structure Formation of Al-Si Alloy Casting Using Cellular Automaton Method. Materials Science Forum, 2008, 575-578, 154-163.	0.3	2
113	Ion Implantation Induced Martensite Nucleation in SUS301 Steel. Nippon Kinzoku Gakkaishi/Journal of the Japan Institute of Metals, 2008, 72, 631-636.	0.4	2
114	Wavelength-dependent magnetic transitions of self-organized iron–aluminum stripes induced by pulsed laser irradiation. Journal of Applied Physics, 2015, 117, .	2.5	2
115	Design of a patterned nanostructure array using a nanosecond pulsed laser. AIP Advances, 2018, 8, 045122.	1.3	2
116	Formation of Stainless Steel Nanoballs via Submerged Glow-discharge Plasma and their Microstructural Analysis with Evaluation of Photocatalytic Activity. ISIJ International, 2018, 58, 1162-1167.	1.4	2
117	Fabrication of Dot-like Nano-protrusions on Silicon Surfaces Using Nanosecond Pulse Nd:YAG Laser Irradiation. Transactions of the Japan Institute of Electronics Packaging, 2010, 3, 57-61.	0.4	2
118	On the ã€^110〉 cylindrical fermi surface and the anisotropic cyclotron resonance peak in lead. Journal of Physics and Chemistry of Solids, 1993, 54, 325-329.	4.0	1
119	Defect-flow-induced heterogeneous dislocation formation and solute redistribution near a grain boundary in austenitic stainless steel under electron irradiation. Journal of Nuclear Materials, 1999, 271-272, 184-188.	2.7	1
120	Formation and Stability of Metallic Silicides during Ion-Beam-Mixing in the Systems of Mo/Si and Ti/Si. Materials Transactions, JIM, 1999, 40, 408-411.	0.9	1
121	Electron-Irradiation-Induced Amorphization in Mo/Si Nano-Multilayer Material. Materials Transactions, 2002, 43, 650-653.	1.2	1
122	Non-equilibrium local phase formation by high-speed deformation in NiTi. Materials Science & Engineering A: Structural Materials: Properties, Microstructure and Processing, 2003, 350, 145-149.	5.6	1
123	Dynamic and static hydrogen effects on mechanical properties in Vanadium alloys. AIP Conference Proceedings, 2006, , .	0.4	1
124	Atomic Structure of Faceted Σ3 CSL Grain Boundary in Silicon: HRTEM and Ab-Initio Calculation. Nippon Kinzoku Gakkaishi/Journal of the Japan Institute of Metals, 2008, 72, 886-891.	0.4	1
125	Effect of growth rate on microstructure and microstructure evolution of directionally solidified Nb-Si alloys. Materials Research Society Symposia Proceedings, 2008, 1128, 53801.	0.1	1
126	Transformation in iron–platinum thin film via nanosecond pulsed laser irradiation. Journal of Physics and Chemistry of Solids, 2017, 109, 46-49.	4.0	1

#	ARTICLE	IF	CITATIONS
127	Misorientation dependence of grain boundary segregation under electron irradiation in an austenitic stainless steel. European Physical Journal Special Topics, 2000, 10, Pr6-173-Pr6-178.	0.2	1
128	Detection of Radiation-Enhanced Diffusion by Means of Neutron-Irradiated Diffusion Couples of Fe-Cr-Ni System. , 2004, , 516-525.		1
129	Precipitation and Amorphization in Boron Carbide Irradiated by High Energy Helium Ions. , 2004, , 670-679.		1
130	Effect of Ion-Irradiation on Phase Transformation in TiNi Shape Memory Alloys. , 2000, , 1147-1158.		1
131	Improvement of Corrosion Resistance and Structural Change in 304 Stainless Steel by means of Ion-Mixing. Materials Transactions, 2002, 43, 638-640.	1.2	Ο
132	Nanostructural Fluctuation in Radiation-Amorphized Alloys. Materials Research Society Symposia Proceedings, 2003, 792, 515.	0.1	0
133	Radiation-Induced Glass Transition and Structural Fluctuation in NiTi Metallic Glass System. AIP Conference Proceedings, 2006, , .	0.4	Ο
134	Fabrication of Quantum Structure Utilizing CSL Boundary by Ion Implantation. Materia Japan, 2008, 47, 638-638.	0.1	0
135	Thermal Stability of Microstructure in Grain Boundary Character Distribution-Optimized and Cold-Worked Austenitic Stainless Steel Developed for Nuclear Reactor Application. Materials Research Society Symposia Proceedings, 2009, 1215, 1.	0.1	0
136	Deformation-induced Amorphization of Crack Tip in NiTi Alloy. Materia Japan, 1998, 37, 372-372.	0.1	0
137	Measurement of Radiation-Induced Segregation by Means of FE-TEM. Materia Japan, 1998, 37, 378-378.	0.1	Ο
138	Ion irradiation technique for electron microscopy. Keikinzoku/Journal of Japan Institute of Light Metals, 2014, 64, 654-662.	0.4	0
139	Advanced Characterization Nanotechnology Platform of Nanotechnology Platform Japan Program in Hokkaido University. Materia Japan, 2019, 58, 758-762.	0.1	0
140	Fabrication of color-toned micro/nanopattern surface by submerged photosynthesis method. Microelectronic Engineering, 2022, 256, 111727.	2.4	0
141	Behavior of Fe-Cr-Ni-xP-yTi Alloys under Electron/He Ion Dual Beam Irradiation. , 1999, , 701-709.		О